COMMUNICATION

Check for updates

Binaphthol-based chiral host molecules for efficient solution-processed circularly polarized OLEDs†

Qiwei Dong,[ab] Chen Xiao,[a] Binghong He,[a] Xuefeng Yang,[c] Songkun Zeng,[a] Qihang Zhong,[a] Pengfei Duan, [iD][c] Weiguo Zhu [iD] *[a] and Yafei Wang [iD] *[a]

Two kinds of chiral hosts, named (*R/S*)-BN-mCP and (*R/S*)-BN-2mCP, are prepared. Solution processable circularly polarized organic light-emitting diodes (CP-OLEDs) based on the chiral hosts and achiral emitter Ir(mypp)$_3$ present the maximum external quantum efficiency (EQE$_{max}$) and dissymmetry factor values (g_{EL}) of 12.7%/-1.7×10^{-3} and 17.1%/-1.3×10^{-3}, respectively. Using (*R*)-BN-2mCP as the chiral host and Ir(mypp)$_3$ and Ir(piq)$_2$(acac) as the achiral emitters, the solution-processed OLED exhibits a broad emission spectrum with the EQE$_{max}$ of 12.1% and g_{EL} of -1.1×10^{-3}.

Circularly polarized organic light-emitting diodes (CP-OLEDs) are favorable for the direct emission of circularly polarized light, and have found great potential applications in optical data storage, optical recognition sensors, quantum computing, optical communication for spintronics and 3D displays.[1,2] Since the first example of CP-OLED was reported by Meijer *et al.* in 1997,[3] great efforts have been devoted to the progress of CP-OLEDs. The most direct and effective strategy to achieve CP-OLEDs is to employ the chiral fluorophore as the emitter in the device. This utility is expected to be maximized by the development of CPL emitters with high brightness and large dissymmetry factor values (*g*). Thus, considerable chiral chromophores including fluorescence, phosphorescence and thermally activated delayed fluorescence (TADF) have been developed. Usually, there are two methods to realize the chiroptical property.

The first strategy is chiral perturbation, where the circularly polarized luminescence (CPL) activities are induced from chiral units directly decorated on the molecular structure.[4–8] The second one is to design chromophores with inherent chirality, in which the chiral elements are constructed by two achiral chromophores hindering rotation in the 3D space.[9–12] For example, our previous work demonstrated an effective chiral phosphorescent emitter *via* introduction of a chiral alkyl chain into the platinum complex skeleton.[13,14] This chiral platinum complex based solution processable CP-OLED achieved the maximum external quantum efficiency (EQE$_{max}$) of above 12% and a |g_{lum}| value of 10^{-2}. Pieters *et al.* firstly reported a TADF emitter enabling circularly polarized light emission through binaphthol chiral perturbation.[4] Unfortunately, both the device performance (EQE$_{max}$: 9.1%) and |g_{lum}| values (1.3×10^{-3}) are not very satisfactory. In the same way, several research groups realized CP-OLEDs based on chiral TADF emitters with EQE$_{max}$ above 30% recently.[7] However, the chiral emitters are usually difficult to synthesize due to the chiral purification. In addition, a chiral emitter is only used for a special device, which has certain limitations in application.

As an alternative method, the host material, having a very important role in OLEDs, can also realize CP-OLEDs through a chiral energy transfer process. Unfortunately, very scarce research has focused on this field to achieve CP-OLEDs.[15,16] Very recently, Yang's group reported a chiral exciplex-forming co-host through employing a chiral donor and an achiral acceptor molecule.[17] Although this device showed a very high EQE$_{max}$ of 33.2% and an acceptable g_{EL} of 2.8×10^{-3}, the device was fabricated *via* a vacuum-deposition method, leading to complicated device structure and high costs.

At the same time as Yang's research, we also proposed a simple and effective method to obtain a chiral host molecule through integrating the classic host 1,3-bis(*N*-carbazolyl)benzene (mCP) moiety into the (*R/S*)-binaphthol ((*R/S*)-BN) chiral skeleton. Thus, two novel chiral hosts (*R/S*)-BN-mCP and (*R/S*)-BN-2mCP were synthesized and prepared (Fig. 1a). Both the chiral

[a] Jiangsu Collaborative Innovation Center of Photovoltaic Science and Engineering, Jiangsu Engineering Laboratory of Light-Electricity-Heat Energy-Converting Materials and Applications, School of Materials Science & Engineering, Changzhou University, Changzhou 213164, China. E-mail: zhuwg18@126.com, qiji830404@hotmail.com

[b] School of Materials Engineering, Changzhou Vocational Institute of Industry Technology, Changzhou 213164, China

[c] CAS Center for Excellence in Nanoscience CAS, Key Laboratory of Nano system and Hierarchical Fabrication National Center for Nanoscience and Technology (NCNST), Beijing 100190, P. R. China

† Electronic supplementary information (ESI) available. See DOI: https://doi.org/10.1039/d2cc06420k

Fig. 1 (a) Molecular structure of the chiral host and achiral emitter; (b) schematic diagram of the solution processable CP-OLED.

compounds exhibit enough high triplet state and intense CPL signals with g_{PL} of 10^{-3}. As expected, the green solution processable CP-OLEDs based on (R)-BN-mCP and (R)-BN-2mCP not only display clearly circularly polarized electroluminescence signals *via* a chiral energy transfer (ET) process (Fig. 1b), but also achieved the EQE_{max} of 12.7% and 17.1%, respectively. Furthermore, using both $Ir(mypp)_3$ and $Ir(piq)_2(acac)$ as the achiral emitter, the (R)-BN-2mCP based solution-processed CP-OLED exhibited a dual-emission band with the EQE_{max} of 12.1% and large g_{EL} of -1.1×10^{-3}. To the best of our knowledge, this is the first example of a solution processable CP-OLED realized by a chiral ET process between the chiral host molecule and achiral emitter.

As shown in Scheme S1 (ESI†), starting from the commercial materials of (R/S)-[1,1′-binaphthalene]-2,2′-diol (R/S)-BN, compound (R/S)-BN-Et was synthesized *via* the nucleophilic substitution reaction in the presence of K_2CO_3. Then, 1,3-dibromo-5-fluorobenzene reacted with (R/S)-BN or (R/S)-BN-Et yielded the key precursors of (R/S)-BN-2Br and (R/S)-BN-4Br by nucleophilic substitution reaction, respectively. Using $Pd_2(dba)_3$ as the catalyst, Buchwald–Hartwig coupling reaction between (R/S)-BN-2Br/(R/S)-BN-4Br and 9H-carbazole provided the target compounds (R/S)-BN-mCP/(R/S)-BN-2mCP which were confirmed by ^1H NMR, ^{13}C NMR, TOF-MS and HPLC (Fig. S1–S22, ESI†). Both compounds exhibit good solubility in ordinary organic solvents, such as toluene, CH_2Cl_2, $CHCl_3$ and THF. Excellent thermal stability was observed with the decomposition

temperature (T_d, at 5 wt% loss weight) detected to be 359 and 524 °C for (R)-BN-mCP and (R)-BN-2mCP, respectively (Fig. S23a, ESI†). The DSC curves obtained during the second heating cycle reveal a relatively high glass transition temperature of 107 and 177 °C for (R)-BN-mCP and (R)-BN-2mCP, respectively (Fig. S23b, ESI†). It is worth noting that one more mCP moiety has a clearly positive effect on the thermal property. Therefore, both the good solubility and thermal property imply that the compounds (R/S)-BN-mCP/(R/S)-BN-2mCP could be suitable for the host materials in OLEDs.

As shown in Fig. S24 (ESI†), both hosts show a twisted molecular configuration, in which large spatial separation between the highest occupied molecular orbital (HOMO) and lowest unoccupied molecular orbital (LUMO) was observed. The LUMO of both compounds is mainly distributed on the chiral binaphthyl skeleton, while the HOMO distributions are mainly governed by the donor carbazole units. Due to the almost identical HOMO and LUMO distributions, both compounds possess similar HOMO/LUMO energy levels. In addition, the triplet energies of (R/S)-BN-mCP and (R/S)-BN-2mCP are evaluated to be 2.57 and 2.67 eV, respectively. In order to further investigate the energy level of the hosts, ultraviolet photoelectron spectra (UPS) were performed for HOMO measurement with the neat film on an ITO substrate. The high-energy and low-energy edges of the UPS spectra of the hosts are depicted in Fig. S25 (ESI†). Based on the cutoff energies obtained using a tangent method, the $E_{HOMO,UPS}$

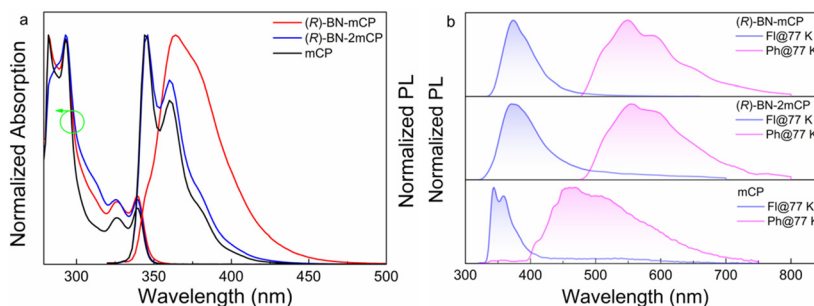**Fig. 2** (a) UV–vis spectra and PL spectra (λ_{ex} = 300 nm) measured in toluene solution (10^{-5} M); (b) fluorescence and phosphorescence in the doped PMMA film (10%) at 77 K temperature (λ_{ex} = 300 nm).

values are calculated to be -5.55 and -5.91 eV for compounds (R)-BN-mCP and (R)-BN-2mCP, respectively. Then, based on the HOMO and optical energy gap, the LUMO energy levels are calculated to be -1.90 and -2.15 eV for compounds (R)-BN-mCP and (R)-BN-2mCP, respectively.

The ultraviolet-visible (UV-vis) absorption and photoluminescent (PL) spectra both in toluene solution and doped PMMA films at room temperature are depicted in Fig. 2, and the relevant data are listed in Table S1 (ESI†). Both hosts exhibit similar absorption spectra with two clear absorption bands from 250 nm to 400 nm (Fig. 2a). The intense absorption bands below 300 nm are assigned to the π–π^* transition of the aromatic backbone, while the weak absorption bands between 320 and 350 nm can be attributed to the intramolecular charge transfer transition. Compared to the prototypical structure, integrating the chiral moiety into the mCP skeleton has a negligible effect on the absorption property. Compound (R)-BN-2mCP shows intense blue emission with fine structured shape both in solution and a doped film, almost identical to the mCP. On the contrary, distinct red-shifted emission spectra with relatively broad and structureless shape are observed for (R)-BN-mCP (Fig. 2a and Fig. S27a, ESI†). The doped PMMA films of (R)-BN-mCP and (R)-BN-2mCP exhibit negligible red shift, implying that the twisted structure can suppress intermolecular interaction (Fig. S27a, ESI†). The low-temperature (77 K) fluorescence (Fl) and phosphorescence (Ph) were carried out in doped PMMA (10 wt%) film (Fig. 2b). According to the onsets of the Fl and Ph spectra, the S_1/T_1 energy levels of (R)-BN-mCP and (R)-BN-2mCP were evaluated to be 3.72/2.61 eV and 3.76/2.67 eV, which is consistent with the DFT calculation results. Such a high triplet energy level can be enough as a host for a green emitter. As depicted in Fig. S27b (ESI†), only mono-exponential decays of 7.95 and 9.35 ns were detected for (R)-BN-mCP and (R)-BN-2mCP in doped PMMA film (10%) at room temperature, respectively, suggesting that the emission originated from the singlet excited state.

The chiroptical properties of (R/S)-BN-mCP and (R/S)-BN-2mCP were investigated using circular dichroism (CD) and circularly polarized photoluminescence spectra, respectively. As depicted in Fig. 3a and b, each enantiomer couple features a mirror image, and the molecules show similar cotton effects at around 300–350 nm due to the same chiral binaphthyl moiety, and the (R/S)-BN-mCP and (R/S)-BN-2mCP enantiomers exhibit identical absorbance at 326 nm and 339 nm. CPL is the emission analog of CD that reflects the chiroptical properties of the luminescent molecules upon excitation. These enantiomers can exhibit clear mirror-image CPL signals in toluene solution with the luminescence dissymmetry factor ($|g_{PL}|$) values of 0.001–0.002 (Fig. 3c and d). Clear CPL signals ($|g_{PL}|$: 10^{-3}) in the Ir(mppy)$_3$ doped host film imply that chirality transfer between the host and guest occurs (Fig. S28, ESI†).

To explore the electroluminescent (EL) property of the chiral hosts, solution-processed OLEDs based on (R/S)-BN-mCP and (R/S)-BN-2mCP were fabricated. Owing to the potential Förster energy transfer (FET) process (Fig. S29, ESI†), green phosphorescence molecule Ir(mppy)$_3$ was chosen as the guest emitter.
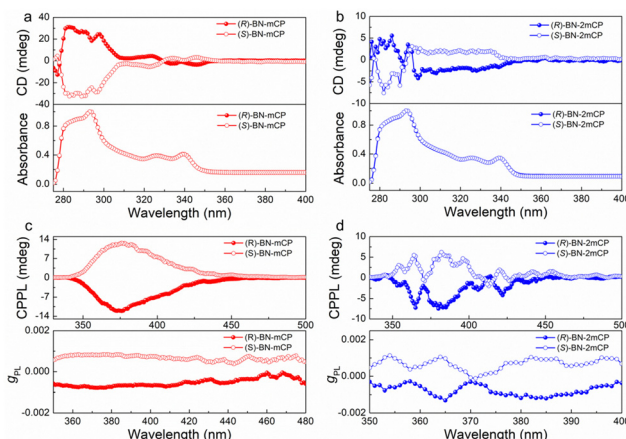

Fig. 3 (a) CD and absorbance spectra of (R/S)-BN-mCP in toluene (10^{-4} M); (b) CD and absorbance spectra of (R/S)-BN-2mCP in toluene (10^{-4} M); (c) CPL and g_{PL} spectra of (R/S)-BN-mCP in toluene (10^{-4} M) (λ_{ex} = 300 nm); (d) CPL and g_{PL} spectra of (R/S)-BN-2mCP in toluene (10^{-4} M) (λ_{ex} = 300 nm).

Therefore, the device configuration is ITO/PEDOT:PSS (40 nm)/hosts: Ir(mppy)$_3$ (20 wt%) (30 nm)/DPEPO (9 nm)/TmPyPB (45 nm)/LiF (0.5 nm)/Al (120 nm). The schematic diagrams of the energy level and chemical structures of the materials in the devices are shown in Fig. S30 (ESI†), and the relevant data are listed in Table S2 (ESI†). Relatively low turn-on voltage (V_{on}@ 1 cd m^{-2}) of 2.8 V was obtained for all devices. Only the typical green emissions from Ir(mppy)$_3$ are observed, suggesting that a complete energy transfer between host and guest occurs. Impressively, both chiral host-based devices display satisfactory performance (Fig. 4a and Fig. S32, ESI†). The maximum external quantum efficiencies (EQE$_{max}$) of 12.7 and 12.4%, and highest luminances (L_{max}) of 5022 and 7230 cd m^{-2} were achieved for (R)-BN-mCP and (S)-BN-mCP based devices, respectively. Owing to the better-balanced carrier transporting
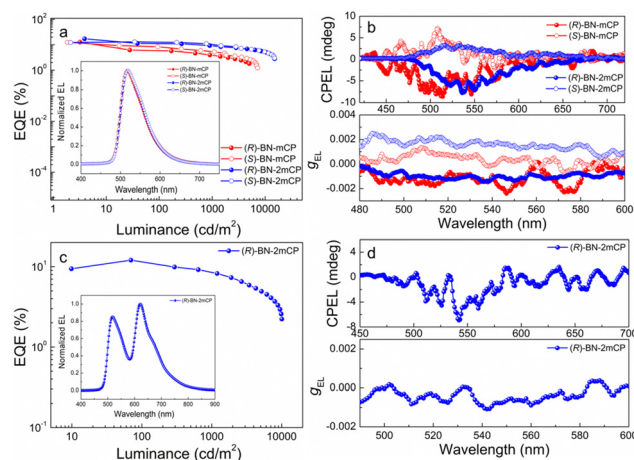

Fig. 4 (a) EQE–luminance curves of the green CP-OLED devices (inset: normalized EL spectra); (b) CPEL spectra and g_{EL} values of the devices *versus* wavelength curves; (c) EQE–luminance curves of the CP-OLED with two emitters (inset: normalized EL spectra) and (d) CPEL spectra and g_{EL} values of the CP-OLED with two emitters *versus* wavelength curves.

property (Fig. S31, ESI†), the (R)-BN-2mCP based device achieved a better performance with the maximum current efficiency (CE) of 61.03 cd A^{-1}, EQE_{max} of 17.1% and L_{max} 15070 cd m^{-2}. Then the CPEL characteristics of the devices with enantiomers were independently measured by using a JASCO CPL-200 under the voltage of 4 V. As illustrated in Fig. 4b, the CP-OLEDs display obvious CPEL signals with opposing g_{EL} of $+1.3 \times 10^{-3}$ for (S)-BN-mCP, -1.7×10^{-3} for (R)-BN-mCP, $+2.1 \times 10^{-3}$ for (S)-BN-2mCP and -1.3×10^{-3} for (R)-BN-2mCP, respectively. As expected, effective circularly polarized EL can be achieved via a chiral ET process from the chiral host molecule to an achiral emitter. Compared to the solution, the CPEL shows a relatively high g value, probably due to the aggregation in the film.[7,18]

Due to its charming performance in a device, compound (R)-BN-2mCP was selected as the host in a multi-emitter device to further explore the chirality transfer. To this end, a solution-processed CP-OLED with two emitters was prepared, in which the phosphorescent $Ir(mppy)_3$ and $Ir(piq)_2(acac)$ were employed as the green and red emitters, respectively. The schematic diagrams of the energy level and chemical structures of the materials in the devices are shown in Fig. S30b (ESI†). As shown in Fig. 4c and Fig. S33, Table S3 (ESI†), the device shows a broad EL spectrum with a dual-emission band. The corresponding CIE coordinates are (0.45, 0.50). A relatively low V_{on} of 3.2 V was detected for the device.

Excellent device performance with the L_{max} of 10060 cd m^{-2}, CE_{max} of 18.56 cd A^{-1} and EQE_{max} of 12.1% was obtained. Correspondingly, this CP-OLED displays a clear CPEL signal with g_{EL} of -1.1×10^{-3}. This result demonstrates that an effective chiral ET process can also occur in the OLED with a multi-emitter layer structure.

In summary, the chiral hosts of (R/S)-BN-mCP and (R/S)-BN-2mCP were designed and synthesized via a combination of the host moiety and a chiral skeleton. This molecular strategy can possess both relatively high triplet state and clear chirality properties. The solution processable CP-OLED based on chiral host (R/S)-BN-mCP and (R/S)-BN-2mCP and achiral phosphorescence achieved the EQE_{max} of 12.7% and 17.1%, concomitant with a large electroluminescence dissymmetry factor of -1.7×10^{-3} and -1.3×10^{-3}, respectively. Furthermore, the (R)-BN-2mCP based solution processable CP-OLED with two achiral phosphorescent emitters exhibited a maximum EQE of 12.1% and the electroluminescence dissymmetry factor of -1.1×10^{-3}. To the best of our knowledge, this is the first example of a chiral host material in a solution processable CP-OLED. This work demonstrated an effective method for realizing efficient solution processable CP-OLEDs via a chiral energy transfer process between a chiral host molecule and achiral emitter.

Conflicts of interest

There are no conflicts to declare.

Notes and references

1 L. Frédéric, A. Desmarchelier, L. Favereau and G. Pieters, *Adv. Funct. Mater.*, 2021, **31**, 2010281.
2 D. Zhang, M. Li and C. Chen, *Chem. Soc. Rev.*, 2020, **49**, 1331–1343.
3 E. Peeters, M. T. Christiaans, R. J. Janssen, H. M. Schoo, H. J. M. Dekkers and E. W. Meijer, *J. Am. Chem. Soc.*, 1997, **119**, 9909–9910.
4 S. Feuillastre, M. Pauton, L. Gao, A. Desmarchelier, A. J. Riives, D. Prim, D. Tondelier, B. Geffroy, G. Muller, G. Clavier and G. Pieters, *J. Am. Chem. Soc.*, 2016, **138**, 3990–3993.
5 Z. P. Yan, K. Liao, H. B. Han, J. Su, Y. X. Zheng and J. L. Zuo, *Chem. Commun.*, 2019, **55**, 8215–8218.
6 Y. Wang, Y. Zhang, W. Hu, Y. Quan, Y. Li and Y. Cheng, *ACS Appl. Mater. Interfaces*, 2019, **11**, 26165–26173.
7 Z. G. Wu, H. B. Han, Z. P. Yan, X. F. Luo, Y. Wang, Y. X. Zheng, J. L. Zuo and Y. Pan, *Adv. Mater.*, 2019, **31**, e1900524.
8 L. Zhou, F. Ni, K. Wang, G. Xie and C. Yang, *Angew. Chem., Int. Ed.*, 2022, **61**, e202203844.
9 M. Li, Y. F. Wang, D. Zhang, L. Duan and C. F. Chen, *Angew. Chem., Int. Ed.*, 2020, **59**, 3500–3504.
10 Z. L. Tu, Z. P. Yan, X. Liang, L. Chen, Z. G. Wu, Y. Wang, Y. X. Zheng, J. L. Zuo and Y. Pan, *Adv. Sci.*, 2020, **7**, 2000804.
11 S. Y. Yang, Y. K. Wang, C. C. Peng, Z. G. Wu, S. Yuan, Y. J. Yu, H. Li, T. T. Wang, H. C. Li, Y. X. Zheng, Z. Q. Jiang and L. S. Liao, *J. Am. Chem. Soc.*, 2020, **142**, 17756–17765.
12 Y. P. Zhang, X. Liang, X. F. Luo, S. Q. Song, S. Li, Y. Wang, Z. P. Mao, W. Y. Xu, Y. X. Zheng, J. L. Zuo and Y. Pan, *Angew. Chem., Int. Ed.*, 2021, **60**, 8435–8440.
13 G. Qian, X. Yang, X. Wang, J. D. Herod, D. W. Bruce, S. Wang, W. Zhu, P. Duan and Y. Wang, *Adv. Opt. Mater.*, 2020, **8**, 2000775.
14 P. Fan, Z. Fang, S. Wang, Q. Dong, C. Xiao, A. J. McEllin, D. W. Bruce, W. Zhu and Y. Wang, *Chin. Chem. Lett.*, 2022, **107934**, 1001–8417.
15 J. Hong, S. Kim, G. Park, Y. Lee, H. Kim, S. Kim, T. W. Lee, C. Kim and Y. You, *Chem. Sci.*, 2021, **12**, 8668–8681.
16 Y. Zhang, Y. Li, Y. Quan, S. Ye and Y. Cheng, *Angew. Chem., Int. Ed.*, 2022, **11**, e202214424.
17 Z. Chen, C. Zhong, J. Han, J. Miao, Y. Qi, Y. Zou, G. Xie, S. Gong and C. Yang, *Adv. Mater.*, 2022, **34**, 2109147.
18 F. Song, Z. Xu, Q. Zhang, Z. Zhao, H. Zhang, W. Zhao, Z. Qiu, C. Qi, H. Zhang, H. H. Y. Sung, I. D. Williams, J. W. Y. Lam, Z. Zhao, A. Qin, D. Ma and B. Z. Tang, *Adv. Funct. Mater.*, 2018, **28**, 1800051.